A Theoretical Study of the Proton-Bound Ammonia Dimer

James A. Platts*

Department of Chemistry, University of Wales, Cardiff, Cardiff CF1 3TB, U.K.

Keith E. Laidig

Department of Medicinal Chemistry, BG-20, University of Washington, Seattle, Washington 98195

Received: December 8, 1994; In Final Form: February 2, 1995®

A detailed investigation into the structure, energetics, and charge distribution of the cation $H_3N-H\cdot\cdot NH_3^+$ is reported. We have employed *ab initio* molecular orbital calculations to investigate the optimal geometry and electronic structure of this and related systems. Using the HF/6-311++G** level of theory, $N_2H_7^+$ is found to be asymmetrically protonated, in line with previous findings. At this level, the hydrogen bond strength is predicted to be 95.8 kJ·mol^{-1}, and the protonation energy of a model "proton sponge" is predicted to be 1051.7 kJ·mol^{-1}. Decomposition of the properties of these systems into atomic contributions, using subsystem quantum mechanics, allows us to identify the underlying reasons for the high stability of $N_2H_7^+$ when compared to its constituents. We show that charge transfer, as well as the proximity of the nitrogens, contributes to the hydrogen bond strength, which ultimately comes from stabilization of the NH_4^+ fragment. We also demonstrate that the high proton affinity of a proton sponge comes solely from the $[N-H\cdot\cdot N]^+$ moiety, with important factors being loss of repulsion between nitrogens and increased electronegativity of nitrogens.

Introduction

Accurate *ab initio* calculations on hydrogen-bonded systems have become common in the literature.[1] Such calculations typically employ large, polarized, and diffuse basis sets and often inclusion of electron correlation. As a result of these calculations, the effects of basis set expansion, correlation, basis set superposition error (BSSE), *etc.*, are reasonably well understood. Allied to such electronic structure calculations, analyses of contributions to the strength and structure of hydrogen bonds have been carried out, *e.g.*, refs 2–4. Coupled with the substantial amount of experimental data[5] in the literature, the conventional hydrogen bond has become a relatively well-understood phenomenon.

By comparison, cationic hydrogen bonds such as proton-bound dimers have been little studied. Early theoretical studies suffered from errors due to small basis sets and lack of electron correlation.[6] In the first study to account for such effects, Del Bene *et al.*[7] found hydrogen bond strengths of 100–140 kJ·mol^{-1} for first-row hydrides. They also showed that basis set size and electron correlation can have significant, qualitative effects on the structure of such complexes; for example, the proton-bound dimer of water has an asymmetrical proton at the Hartree–Fock level but a symmetrical one when correlation is included. Since this study, however, only a few further such studies have been published.[8,9] Moreover, little or no interest has been focused upon analysis of the contributions to the stability of such systems, despite the possibility that they may play an important role in biological systems.

Cationic hydrogen bonds are of great importance in the field of "proton sponges", generally organic molecules with very high proton affinities and pK_a's but low kinetic basicities.[10] These generally involve the cooperative effect of two basic centers, usually amines, acting to make protonation very energetically favorable. Obviously, the characteristics of the hydrogen bond so formed will play a significant role in determining the basicity

of a given proton sponge, as will other factors such as relief of strain upon protonation. Attempts to quantify such effects in proton sponges have been hindered by the lack of information in the literature on the nature of the $[N-H\cdot\cdot N]^+$ interaction. This, coupled with the inherent interest in such strongly bound systems, is the motivation behind the work reported here: we wish to probe in detail this type of interaction with the aim of identifying the origin of its relative stability.

With this in mind, we have undertaken a study of the simplest model of this interaction, the $N_2H_7^+$ cation. In all work on this cation since 1985,[7,11] it was found to have C_{3v} symmetry (asymmetrical proton) at all levels of theory considered (up to MP4SDQ/6-31G**). Further evidence for the asymmetrical positioning of the proton in this cation seems to come from single-crystal X-ray diffraction.[12] Importantly for this study, electron correlation was found to have no qualitative effect upon the cation's structure, unlike in the case of the $H_5O_2^+$ cation. Consequently, we have limited the calculations reported here to the Hartree–Fock level, making further analysis computationally feasible.

We have employed subsystem quantum mechanics as implemented in the theory of Atoms in Molecules, as developed by Bader and co-workers,[13] in our attempt to gain insight into this interaction. This theory is based around the formal definition of a quantum mechanical subsystem, one which obeys the same laws as does the total system in quantum mechanics. Bader has shown that such a subsystem is defined by the "zero-flux surface", *i.e.*, the surface in real space which obeys the equation

$$\nabla\varrho(\mathbf{r})\cdot\mathbf{n}(\mathbf{r}) = 0 \qquad (1)$$

for all points on the surface. This surface condition can be thought of as the subsystem analogue of the "natural boundary conditions" required in Schrödinger's quantum mechanics.[14] Bader has demonstrated that the properties of quantum mechanical subsystems behave in the same fashion as those expected of the "atoms of chemistry". We use the term "atom"
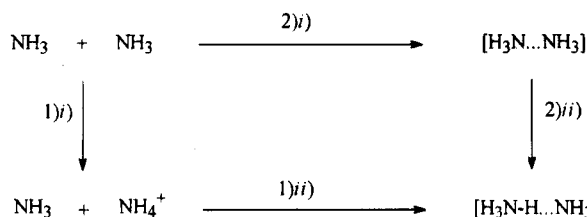
Figure 1. Hypothetical reaction scheme from NH_3 + NH_3 to $N_2H_7^+$.

in all that follows purely as a less unwieldy synonym for "quantum mechanical subsystem".

The extraction of chemically interesting information from subsystem quantum mechanics lies not simply in the bare definition of an atom. Having identified the region of space bound by the zero-flux surface, it is then possible to obtain atomic properties. This is done by integrating "property densities" over each atomic region. The property density corresponding to an observable A, $\varrho_A(\mathbf{r})$, is given by

$$\varrho_A(\mathbf{r}) = \frac{N}{2} \int d\tau' \, (\psi^* \hat{A} \psi + (\hat{A}\psi)^* \psi) \qquad (2)$$

where $d\tau'$ means integration over all spin coordinates and all position coordinates but one. From this property density, an atomic property is obtained from

$$A(\Omega) = \int_\Omega d\tau \, \varrho_A(\mathbf{r}) \qquad (3)$$

It has been repeatedly shown that such atomic properties yield the total molecular properties when summed over all atoms. Atomic properties commonly reported include populations (and hence charges),[15,16] energies (including kinetic and potential contributions),[2,17] atomic volumes,[18] atomic dipole and quadrupole moments,[19] polarizabilities,[20] and magnetic susceptibilities.[21] These properties, and their changes on chemical processes, reveal a great deal about the chemistry of the system under investigation.

We have performed this type of analysis on the $N_2H_7^+$ cation and on the related systems NH_3, NH_4^+, and $[H_3N\cdots NH_3]$, concentrating on the changes in atomic properties upon the various steps in the formation of $N_2H_7^+$ from 2(NH_3). The latter was chosen as a model of proton sponges, with the nitrogen lone pairs pointing toward each other. This is not stable relative to two ammonia molecules, but we feel its inclusion is justified due to its relation to proton sponges. The two possible pathways from $(NH_3)_2$ to $N_2H_7^+$ are summarized in Figure 1. Path 1 involves protonation of ammonia, followed by hydrogen bond formation; path 2 is the association of two ammonia molecules, forming the proton sponge analogue, which is then protonated.

Computation

All MO calculations employed the GAUSSIAN92 package,[22] running on an IBM/RS6000. Geometry optimizations were carried out at the HF/6-311++G**[23] level of theory. Molecular energies and charge distributions were calculated at the same level as the optimizations in order to avoid non-zero Hellmann–Feynman forces making unknown contributions to atomic properties. Throughout all calculations, NH_4^+ was constrained to have T_d symmetry, N_2H_6 to have D_{3d}, $N_2H_7^+$ to have C_s, and NH_3 to have C_{3v} symmetry. In the case of $[H_3N\cdots NH_3]$, the $N\cdots N$ internuclear distance was fixed at that found for $N_2H_7^+$ and all other parameters optimized. Molecular dipole moments have been calculated, taking the origin to be the molecular center of mass. The molecules have been oriented such that the z axis lies along the N...N axis (the N lone pair axis in ammonia),

TABLE 1: HF/6-311++G Molecular Properties**

	NH_3	NH_4^+	N_2H_6	$N_2H_7^+$
$r(N\cdots N)$, Å			2.822	2.822
$r(N-H)^a$	1.000		1.001	1.005
$r(N-H)'$		1.012		1.009
$r(N-H)''$				1.056
E, au	−56.214 75	−56.559 19	−112.409 88	−112.810 44
D_z, au	−0.6765	0.0000	0.0000	−1.2210

^{a} $r(N-H)$ is an ammonia-type N−H bond; $r(N-H)'$ is an ammonium-type N−H bond; $r(N-H)''$ is a H-bonding N−H bond.

except NH_4^+ which obviously has no unique axis of symmetry. In NH_3, the positive z-axis direction is from H to N, while in $N_2H_7^+$ this is from NH_4^+ to NH_3. Decomposition of the molecular charge distributions so obtained was performed with the AIMPAC suite of programs.[16] In particular, the critical point analysis program EXTREME and the properties of atoms in molecules program PROAIM were used. Atomic energies have been corrected for the virial defect, $i.e.$, the deviation from 2 of the ratio $-V/T$ caused by the use of a finite basis set.

Results

Results for the total system optimizations are reported in Table 1. The geometrical results are close to HF structures reported previously, and as noted above, electron correlation effects do not qualitatively change this structure. The optimum $N\cdots N$ distance of 2.822 Å in $N_2H_7^+$ is appreciably longer than the solid-state value of 2.69(5) Å found from X-ray diffraction but agrees with earlier theoretical predictions.[7,11b] We find that $r(N-H)$ increases on protonation of ammonia, step 1i, and the N−H bond involved in hydrogen bonding lengthens further on formation of the hydrogen bond, step 1ii.

The energies of the various systems in Table 1 reveal a total change on going from $2NH_3$ to $N_2H_7^+$ of 1000.2 kJ·mol^{-1} (1 kJ·mol^{-1} = 0.239 kcal·mol^{-1}) and result in a proton affinity of ammonia of 904.3 kJ·mol^{-1} and a hydrogen bond strength of 95.8 kJ·mol^{-1}. As these are corrected neither for zero-point energy changes nor basis set superposition error, they are certainly overestimates. Ikuta found such corrections to be small for hydrogen bond formation, and we believe our value for the hydrogen bond strength is close enough to his corrected values[11b] to be reasonable for the purposes of this discussion. The energy change for step 2i, formation of the proton sponge analogue from two ammonia molecules (with an $N\cdots N$ distance of 2.822 Å), is +51.5 kJ·mol^{-1}, which can be taken as an estimate of the repulsion between nitrogens in a proton sponge. Protonation of N_2H_6 results in a stabilization of 1051.7 kJ·mol^{-1}, comparable with 1082.2 kJ·mol^{-1} found for the protonation of a proton sponge.[10c] The total dipole moments of the molecules and complexes are also reported in Table 1 (note that a dipole is defined to point from the negative to the positive pole). We find that NH_3 has a dipole moment of 0.677 a.u. from N to H, while that of $N_2H_7^+$ is considerably larger at 1.221 a.u. (both NH_4^+ and N_2H_6 have zero dipole moment due to their symmetry). The dipole moment of a cation is origin dependent, and this value for $N_2H_7^+$ was calculated using the center of mass as the origin, which lies approximately midway between NH_3 and NH_4^+. Hence, the large dipole moment of $N_2H_7^+$ is due simply to the separation of charge about the origin in this coordinate frame.

The properties determined at the (3, −1) critical point (CP), the minimum on the line of maximal charge density joining two atoms, are listed in Table 2. The properties evaluated at such points have been shown to be a powerful and efficient method for investigation of bonding and atomic interactions.[24]

Study of the Proton-Bound Ammonia Dimer

J. Phys. Chem., Vol. 99, No. 17, 1995 **6489**

TABLE 2: Bond Critical Properties[a]

	ϱ	$\nabla^2\varrho$	ϵ	r_A	r_B
		NH_3			
N−H	0.3525	−1.7633	0.0479	1.3879	0.5024
		NH_4^+			
N−H	0.3444	−2.1566	0.0000	1.4756	0.4365
		N_2H_6			
N···N	0.0174	+0.0581	0.0000	2.6664	2.6664
N−H	0.3513	−1.7167	0.0523	1.3831	0.5087
		$N_2H_7^+$			
N2−H1	0.3477	−2.0784	0.0058	1.4546	0.4516
N2−H3	0.2964	−1.9444	0.0000	1.5966	0.3997
N2−H6,7	0.3477	−2.0781	0.0058	1.4546	0.4516
N4···H3	0.0468	+0.0964	0.0000	2.3080	1.0285
N4−H5	0.3488	−1.8271	0.0314	1.4101	0.4890
N4−H8,9	0.3488	−1.8268	0.0314	1.4101	0.4891

[a] ϱ is the value of the charge density at the critical point; $\nabla^2\varrho$ is the second derivative of the density here; ϵ is the ellipticity of the bond, defined as 1 − the ratio of the two negative curvatures of the charge density; r_A and r_B are the distances of the critical point from nuclei A and B in the bond A−B.

TABLE 3: Atomic Properties of NH_3 and NH_4^+[a]

	N1	H2,3,4	H5
		NH_3	
N	8.0824	0.6392	
E	−54.7728	−0.4806	
V_{NE}[b]	−145.9885	−3.3567	
V_{NEO}	−133.7627	−0.9620	
V_{REP}	+36.4420	+2.3953	
M_z	−0.2028	+0.0818	
M_Ω	0.2028	0.1885	
Q_{zz}	−5.9656	−0.3139	
		NH_4^+	
N	8.1224	0.4694	0.4694
E	−55.0071	−0.3880	−0.3880
V_{NE}	−151.1411	−2.6608	−2.6608
V_{NEO}	−134.6172	−0.7729	−0.7729
V_{REP}	+41.1247	+1.8846	+1.8846
M_z	0.0000	+0.0443	−0.1329
M_Ω	0.0000	0.1329	0.1329
Q_{zz}	−4.4424	−0.1799	−0.1507

[a] All values are in atomic units. [b] V_{NE} is the total electron−nuclear potential energy of each atom; V_{NEO} is the electron−nuclear potential energy within each atom's basin; V_{REP} is the total repulsive potential energy of each atom.

The high value of the density and its negative Laplacian in the N−H bond of ammonia indicate that this is a typical covalent bond. The bonded radii indicate that the critical point lies close to the hydrogen, a result of the greater electronegativity of nitrogen. Protonation causes a loss of density from the N−H bond CP but an increase in the negative Laplacian value. Protonation also allows nitrogen to expand by almost 0.1 a.u., since the presence of interatomic stabilization with the proton allows N to accept more density. Bringing two ammonia molecules together causes a small change in the opposite direction: N−H bonds becoming weaker and hydrogens becoming larger. The N−H bonding in $N_2H_7^+$ is hardly changed in the outer regions, but in the N−H···N part, we observe an accumulation of charge in the hydrogen-bonded region (around twice that found in conventional hydrogen bonding[2]) and a weakening of the N−H bond, an effect experimentally observed in the N−H stretching frequency in IR spectroscopy.[4,5]

Table 3 contains the properties of the atoms in ammonia, obtained from the property density integration method outlined above. The populations, $N(\Omega)$, of the atoms in ammonia show that charge is transferred from N to H to the extent that N has

a charge of −1.082 e. We have broken down the total nuclear−electron potential energy into the attraction of a nucleus for the charge density contained within its own basin, V_{NEO}, and the attractions between nuclei and charges in separate basins, V_{NE} − V_{NEO}. These components of the atomic potential energies show that the major stabilization of nitrogen comes from its own intraatomic interactions, V_{NEO}, while that of the hydrogens is due to interatomic stabilizations. The negative value of nitrogen's z axis first moment reveals that the electron density within nitrogen's basin has its centroid displaced away from the hydrogens (the atomic first moment is a measure of the dipolar polarization of an atom's charge density in that it points from the centroid of negative charge to that of positive charge). This is in the opposite direction to that expected on the basis of charge transfer and is a result of the lone pair density on nitrogen outweighing the effects of charge separation. The most negative component of nitrogen's second moments is Y_{zz}, meaning that charge is preferentially concentrated along the z axis. The hydrogens have only a small polarization away from N, a product of the charge transfer to nitrogen.

Atomic properties of $N_2H_7^+$, and the two intermediates in the hypothetical reaction scheme leading to it, are reported in Tables 3 and 4. Considering route 1 (protonation followed by hydrogen bond formation) first, we see that the dominating change on protonation of ammonia (Table 3) is a substantial (0.469 e) charge transfer to the new hydrogen, H5. This charge is transferred from the NH_3 H's via the nitrogen, since N1 is the only atom to share an interatomic surface with H5. An increase in the population of N1 is also observed, again due to charge transfer from the original hydrogens. This results in an overall stabilization of N1 as well as H5, balanced by a destabilization of the original hydrogens. The fact that in all atoms the change in (V_{NE} − V_{NEO}) is much larger than that in V_{NEO} demonstrates that interatomic effects dominate these energy changes.

The atomic first moments in the ammonium ion reveal a depolarization of N1 along the z axis relative to ammonia. This depolarization is caused by the loss of the lone pair density upon protonation (the symmetry of the molecule means that there is now no distortion of nitrogen's charge in any one direction). The original hydrogens are also depolarized relative to ammonia and in a direction toward nitrogen. Since nitrogen is actually more negative here, this must be due to the competing attraction of their electron densities for the attached proton. Changes in z axis second moments show a large depolarization of N along z, a result of the loss of lone pair density to the new hydrogen.

Hydrogen bond formation between NH_3 and NH_4^+ has a large effect on the calculated atomic properties (Table 4; see Figure 2 for numbering scheme used). All atoms have significant changes in their populations (see Figure 3); the largest of these are found in the [N−H···N]$^+$ moiety. H3, the hydrogen participating in the hydrogen bond, loses 0.085 e, but all other atoms in the NH_4^+ fragment gain in population, resulting in a total charge transfer of 0.072 e from NH_3 to NH_4^+. The NH_3 fragment loses this charge in spite of the gain in density experienced by N4, implying that charge redistribution within the constituents plays a part in determining the stability of the dimer.

The approach of the two fragments causes large increases in both the attractive and repulsive potential energies of all atoms, with changes as large as 17.682 hartrees in these properties. Obviously, since $N_2H_7^+$ is bound with respect to its constituent molecules, the increased attraction is greater than the increased repulsion (case I in Bader's[15b] terminology). The stabilization

TABLE 4: Atomic Properties of N_2H_6 and $N_2H_7^+$

	H1	N2	H3	N4	H5	H6,7	H8,H9
			N_2H_6				
N	0.6570	8.0288		8.0288	0.6570	0.6570	0.6570
E	−0.4874	−54.7428		−54.7428	−0.4874	−0.4874	−0.4874
V_{NE}	−4.4116	−160.1707		−160.1707	−4.4116	−4.4116	−4.4116
V_{NEO}	−0.9776	−133.5935		−133.5935	−0.9776	−0.9776	−0.9776
V_{REP}	+3.4374	+50.6904		+50.9604	+3.4374	+3.4374	+3.4374
M_z	−0.0908	−0.0032		−0.0032	+0.0908	−0.0908	+0.0908
M_Ω	0.1979	0.0032		0.0032	0.1979	0.1979	0.1979
Q_{zz}	−0.3378	−5.4897		−5.4897	−0.3378	−0.3378	−0.3378
			$N_2H_7^+$				
N	0.5042	8.1744	0.3848	8.1542	0.5913	0.5043	0.5913
E	−0.4085	−55.0456	−0.3238	−54.8487	−0.4556	−0.4085	−0.4556
V_{NE}	−3.6028	−165.9491	−3.2531	−163.6700	−4.1356	−3.6024	−4.1363
V_{NEO}	−0.8148	−134.8037	−0.5429	−134.1976	−0.9112	−0.8148	−0.9112
V_{REP}	+2.7856	+55.8548	+2.6054	+53.9696	+3.2240	+2.7852	+3.2247
M_z	+0.0496	−0.1191	−0.0974	+0.1697	−0.0713	+0.0500	−0.0711
M_Ω	0.1419	0.1191	0.0974	0.1697	0.1688	0.1418	0.1688
Q_{zz}	−0.2017	−4.7301	−0.0696	−5.3107	−0.2642	−0.2016	−0.2643
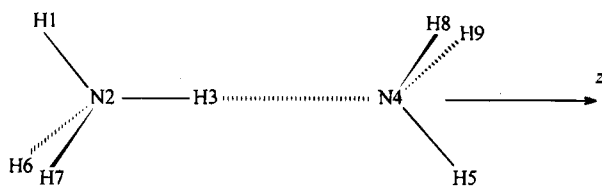
Figure 2. Atom numbering and z axis used for $N_2H_7^+$.
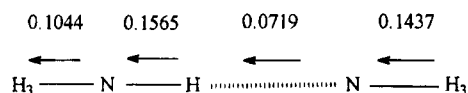
Step 1) *ii)*
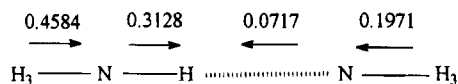
Step 2) *ii)*

Figure 3. Atomic population changes on steps 1ii and 2ii: The direction of the arrows signify the direction of charge transfer.

of the dimer occurs mainly in the NH_4^+ fragment, whose energy falls by 0.036 hartrees (94.0 kJ·mol⁻¹). N4's stabilization due to its proximity to NH_4^+ is offset by the destabilization of the attached hydrogens, resulting in a total stabilization of NH_3 of just 0.001 hartrees (2.4 kJ·mol⁻¹). Interestingly, those atoms which are stabilized overall have increased stabilization within their own basins, suggesting that despite the seemingly dominant role of interatomic effects, intraatomic effects may play a significant part in tipping the balance of attractive and repulsive forces.

By far the greatest change in atomic first moments on hydrogen bond formation occurs in N2, whose centroid of charge is shifted along the positive z direction toward H3 and N4. A smaller depolarization in the same direction is observed in N4. All hydrogens, however, have polarizations in the opposite direction to this. On the basis of the observed charge transfer from base to acid on hydrogen bond formation (Figure 3), one may expect the atomic first moments to show positive changes in the z axis, *i.e.*, a shift in each atom's density in the negative z direction. This is indeed observed for the hydrogens, which polarize in the opposite direction to the charge transfer. The nitrogens, on the other hand, do not follow this pattern;

N2's density is centered toward the highly positively charged H3, an arrangement of charge which allows the greatest stabilization of these atoms. The atomic dipole of N4 is dominated by the presence of the lone pair, as noted in the discussion of ammonia's atomic properties above. Hydrogen bond formation causes some of this density to be transferred to H3, resulting in a reduction of nitrogen's first moment. These changes in atomic properties are small in comparison with the large change in the total dipole moment on hydrogen bond formation. In fact, the direction of charge transfer is from NH_3 to NH_4^+, which actually acts to reduce the dipole moment of $N_2H_7^+$. This charge transfer only partially offsets the effect of charge separation about the origin. Second moment changes are found to be greatest in the nitrogens; N2 has a quadrupole polarization along the z axis, while N4, however, undergoes a large depolarization in this same direction. As in the atomic dipole changes, these changes have their origin in the charge transfer from base to acid: N4 loses some of its lone pair density and is therefore depolarized in this direction. Density is accepted by N2, which can be polarized away from its tetrahedral symmetry in NH_4^+.

Route 2 in the formation of $N_2H_7^+$, via the proton sponge analogue N_2H_6, is an even less studied process than is route 1. Bringing two ammonia molecules together results in a destabilization; the decomposition of the total properties of N_2H_6 in Table 3 shows that this is due to destabilization of the nitrogens, which lose out in terms of population and energy. This is clearly indicative of the repulsion between the negatively charged nitrogens, a destabilizing influence which the system tries to minimize by moving charge away from the N···N region. As there is no change in the total population of the system in this step, the charge lost by the nitrogens must move into the basins of the attached hydrogens. Table 2 shows that the bonded radius of such hydrogens hardly increases at all, so their increase in population must be due to charge redistribution. This repulsion between nitrogens is apparent in their first moments; both are found to be highly depolarized when compared with isolated ammonia. This is again indicative of the removal of density from the N···N region, a result of the "squashing" of the charge density here. This can also be seen in the second moments, which show a strong quadrupolar depolarization of the nitrogens out of the z axis. Step 2i is the reverse of case I, with large increases in attractive and repulsive energies. Unlike step 1ii, the repulsion dominates here, and the system is not bound relative to its constituent monomers.

Protonation of N_2H_6, step 2ii, results in a stabilization of 1051.7 kJ·mol⁻¹. Table 4 shows that all the stabilization energy

Study of the Proton-Bound Ammonia Dimer

J. Phys. Chem., Vol. 99, No. 17, 1995 **6491**

comes from N2, H3, and N4 (the total stabilization of these three atoms is 1923.2 kJ·mol^{-1}), with the outer hydrogens' destabilization balanced against this. As in protonation of ammonia, the largest energy gain is found in the added hydrogen; its withdrawal of 0.385 e from its surroundings results in it being stabilized by 0.324 hartrees. This is rather less than found in the protonation of NH$_3$, as is the population of the new proton. Both nitrogens also have substantial increases in their populations, gaining much more charge than was lost on formation of N$_2$H$_6$. This causes stabilization of both, N2 almost as much as the new hydrogen and considerably more than in step 1i. The energy changes in the [N$-$H··N]$^+$ region are dominated by interatomic stabilizations caused by the proximity of the negatively charged nitrogens and the positively charged hydrogen. Protonation removes the repulsive interaction of the nitrogens in N$_2$H$_6$, creating attractive forces between them and the hydrogen. The influence of H3 means that more density in the basins of the nitrogens can be stabilized, and hence, the nitrogens are effectively more electronegative than in ammonia. This effect is clearly seen in the dipoles of the nitrogens; protonation causes the centroid of charge in each nitrogen to move toward the central hydrogen, *i.e.*, in the direction found to be preferred in ammonia. Despite this repolarization of the nitrogens, their second moments are decreased relative to N$_2$H$_6$.

The outer hydrogens actually undergo a decrease in their inter- and intraatomic stabilizations, despite the addition of a proton. This must be due to the large loss of charge experienced by these atoms, meaning a reduction in the stabilizing interaction between the electron density of the hydrogens and the nitrogen nuclei to which they are attached. This is also evident in the reduction of the repulsive energy of these atoms. All the outer hydrogens are destabilized, counteracting the large stabilization of the [N$-$H··N]$^+$ moiety. Overall, the energy changes show that protonation stabilizes the NH$_3$ fragment which is protonated by 1023.7 kJ·mol^{-1} and the remaining NH$_3$ fragment by only 27.6 kJ·mol^{-1}.

Discussion

The atomic properties reported here reveal a picture of a hydrogen bond whose stability is due almost entirely to the stabilization of the acidic fragment. This is not due simply to its proximity to the base, although this is undeniably an important factor as can be seen in the larger changes in ($V_{NE} - V_{NEO}$) than in those observed in V_{NEO}. The substantial transfer of electron density from base to acid, larger than that found for neutral hydrogen bonding, will also tend to stabilize the acid. Despite this charge transfer, the base fragment is (very slightly) stabilized. This is made possible by the internal rearrangement of charge within NH$_3$ in order to get as much density as close as possible to the acid, *i.e.*, by a large transfer from H to N. This can be thought of as an increase in the electronegativity of N, allowed by the proximity of the acid which can act to stabilize the extra charge on the basic N. Thus, despite the vast majority of the stabilization coming from the NH$_4^+$ fragment, the ability of NH$_3$ to rearrange its charge distribution in this manner plays an important role in determining the large hydrogen bond strength. This also suggests that a more easily polarized base, which would allow greater charge transfer to N (perhaps NMe$_3$),[10d] may form a stronger hydrogen bond with NH$_4^+$ than does NH$_3$.

The most strongly bound complex discussed by Carroll and Bader[2] was H$_3$N··HF, with a hydrogen bond strength of 46.2 kJ·mol^{-1} at the same level of theory used here. Comparison of their results for this complex with those presented here allows us to investigate how, if at all, the cationic system differs from

neutral hydrogen bonding. In general, we find the patterns in the properties are similar for the two systems, with slightly larger changes in N$_2$H$_7^+$. For example, the value of ϱ at the hydrogen bond critical point is 0.034 e·bohr^{-3} in H$_3$N··HF and 0.047 in N$_2$H$_7^+$; 0.046 e of charge is transferred from NH$_3$ to HF, compared with 0.072 e to NH$_4^+$. One major difference from our results is in the loss of charge from the central hydrogen, only 0.020 e in H$_3$N··HF. This difference may well be due to the higher positive charge of hydrogen in HF relative to NH$_4^+$, resulting in less density being available to be lost. However, in almost every property considered, there is no qualitative difference between the two hydrogen bonds, suggesting that the charged hydrogen bond is different only in degree, rather than in nature, to neutral hydrogen bonds.

Our model for the protonation of a proton sponge provides much insight into a hitherto poorly understood process. We have obtained a rough estimate of the repulsion between the nitrogens in such a molecule of around 50 kJ·mol^{-1}. This will obviously be removed upon protonation; the relief of this repulsion thus makes a contribution to the proton affinity of a proton sponge, a contribution which may well be greater than this estimate for the tertiary amines commonly found in these molecules. Atomic properties show that the proton affinity of N$_2$H$_6$ is enhanced relative to NH$_3$ despite the lesser stabilization of the added proton. This is more than compensated for by the increased stabilizations in the nitrogen to which the proton attaches and in the nitrogen of NH$_3$. This, it seems, is the origin of the high proton affinity: the protonated nitrogen is more electronegative than in a simple amine, allowing it to accept more change than in the protonation of a simple amine. Similarly, the proximity of the basic nitrogen to the acidic hydrogen allows it to stabilize more density within its own basin than in isolated ammonia.

Conclusions

The detailed investigation into N$_2$H$_7^+$ and related systems reported here has allowed us to identify atomic and molecular properties crucial to the stability of the cation. Our calculations shed new light on, and give insight into, processes related to these systems. In particular, we have estimated the effect of repulsive interactions in proton sponges and shown it to be of considerable importance in their protonation. Furthermore, we have found the origin of this repulsion to lie in the large depolarization of the nitrogens along the N··N axis and in their resulting loss of charge. We have identified those regions of the molecules in which the overall stabilization occurs; in hydrogen bond formation, we have shown that the energy drop is almost exclusively concentrated in the NH$_4^+$ fragment, while in protonation all the stabilization comes from the [N$-$H··N]$^+$ moiety. Finally, we have demonstrated that such cationic hydrogen bonds do not show any qualitative differences from neutral hydrogen bonding.

References and Notes

(1) See for example: (a) Frisch, M. J.; Pople, J. A.; Del Bene, J. E. *J. Phys. Chem.* **1985**, *89*, 3664 and references cited therein. (b) Frisch, M. J.; Del Bene, J. E.; Binkley, J. S.; Schaefer, H. F., III. *J. Chem. Phys.* **1986**, *84*, 2279. (c) Schaefer, H. F., III; Yamaguchi, Y. *THEOCHEM* **1986**, *135*, 369. (d) Del Bene, J. E. *J. Chem. Phys.* **1987**, *86*, 2110. (e) Latajka, Z.; Scheiner, S. *Chem. Phys.* **1988**, *122*, 413. (f) Kim, K. S.; Mhin, B. J.; Choi, U. S.; Lee, K. *J. Chem. Phys.* **1992**, *97*, 6649. (g) Bacskay, G. B.

Mol. Phys. **1992**, *77*, 61. (h) Saebo, S.; Tong, W.; Pulay, P. *J. Chem. Phys.* **1993**, *98*, 2170. (i) Dobado, J. A.; Molina, J. M. *J. Phys. Chem.* **1993**, *97*, 11415.

(2) Carroll, M. T.; Bader, R. F. W. *Mol. Phys.* **1988**, *65*, 695.

(3) Morokuma, K. *Acc. Chem. Res.* **1977**, *10*, 294.

(4) Schuster, P.; Zundel, G.; Sandorfly, C. Eds. *The Hydrogen Bond*; North Holland: Amsterdam, 1976.

(5) Legon, A. C.; Millen, D. J. *Chem. Rev.* **1986**, *86*, 635 and references cited therein.

(6) Desmeules, P. J.; Allen, L. C. *J. Chem. Phys.* **1980**, *72*, 4731.

(7) Del Bene, J. E.; Frisch, M. J.; Pople, J. A. *J. Phys. Chem.* **1985**, *89*, 3669.

(8) Xie, Y. M.; Remington, R. B.; Schaefer, H. F., III. *J. Chem. Phys.* **1994**, *101*, 4878.

(9) Del Bene, J. E. *Int. J. Quant. Chem.* **1988**, *S15*, 119.

(10) (a) Alder, R. W. *Chem. Rev.* **1989**, *89*, 1215. (b) Staab, H. A.; Saupe, T. *Angew. Chem., Int. Ed. Engl.* **1988**, *27*, 865. (c) Platts, J. A.; Howard, S. T.; Wozniak, K. *J. Org. Chem.* **1994**, *59*, 4647. (d) Howard, S. T.; Platts, J. A.; Alder, R. W. In preparation.

(11) (a) Del Bene, J. E. *J. Comput. Chem.* **1987**, *8*, 810. (b) Ikuta, S. *J. Chem. Phys.* **1987**, *87*, 1900. (c) Jaroszewski, L.; Leysng, B.; Tanner, J. J.; McCammon, J. A. *Chem. Phys. Lett.* **1990**, *175*, 282.

(12) Berthold, H. J.; Preibsch, W.; Vonholdt, E. *Angew. Chem., Int. Ed. Engl.* **1988**, *27*, 1524.

(13) (a) Bader, R. F. W.; Nguyen-Dang, T. T. *Adv. Quant. Chem.* **1981**, *14*, 63. (b) Bader, R. F. W. *Atoms in Molecules; A Quantum Theory*; Oxford University: Oxford, 1990. (c) Bader, R. F. W. *Chem. Rev.* **1991**, *91*, 893.

(14) Courant, R.; Hilbert, D. *Methods of Mathematical Physics*; Wiley: Interscience: New York, 1953; Vol. 1.

(15) (a) Bader, R. F. W.; Cheeseman, J. R.; Laidig, K. E.; Wiberg, K. B.; Breneman, C. *J. Am. Chem. Soc.* **1990**, *112*, 6530. (b) Bader, R. F. W.; Zou, P. F. *Chem. Phys. Lett.* **1992**, *91*, 54. (c) Glaser, R.; Choy, G. S.-C. *J. Am. Chem. Soc.* **1993**, *115*, 2340.

(16) Biegler-König, F. W.; Bader, R. F. W.; Tang, T. H. *J. Comput. Chem.* **1982**, *3*, 317.

(17) Bader, R. F. W.; Chang, C. *J. Phys. Chem.* **1989**, *93*, 5095.

(18) Bader, R. F. W.; Carroll, M. T.; Cheeseman, J. R.; Chang, C. *J. Am. Chem. Soc.* **1989**, *109*, 7968.

(19) (a) Bader, R. F. W.; Larouche, A.; Gatti, C.; Carroll, M. T.; MacDougall, P. J.; Wiberg, K. B. *J. Chem. Phys.* **1987**, *87*, 1142. (b) Laidig, K. E. *Chem. Phys. Lett.* **1994**, *225*, 285.

(20) Laidig, K. E.; Bader, R. F. W. *J. Chem. Phys.* **1990**, *93*, 7213.

(21) (a) Keith, T. A.; Bader, R. F. W. *Chem. Phys. Lett.* **1993**, *210*, 223. (b) Bader, R. F. W.; Keith, T. A. *J. Chem. Phys.* **1993**, *99*, 3683.

(22) Frisch, M. J.; Trucks, G. W.; Head-Gordon, M.; Gill, P. M. W.; Wong, M. W.; Foresman, J. B.; Gonzalez, C.; Martin, R. L.; Fox, D. J.; Defrees, D. J.; Baker, J.; Stewart, J. J. P.; Pople, J. A. *Gaussian 92, Revision B*; Gaussian Inc.: Pittsburgh, PA, 1992.

(23) (a) Krishnan, R.; Binkley, J. S.; Pople, J. A. *J. Chem. Phys.* **1980**, *72*, 650. (b) Hariharan, P. C.; Pople, J. A. *Theor. Chim. Acta* **1973**, *28*, 213. (c) Frisch, M. J.; Pople, J. A.; Binkley, J. S. *J. Chem. Phys.* **1984**, *80*, 3265.

(24) Bader, R. F. W.; Essen, H. *J. Chem. Phys.* **1984**, *80*, 1943.